

## Research paper

# Periodic and chaotic psychological stress variations as predicted by a social support buffered response model



Richard J. Field<sup>a</sup>, Jason A.C. Gallas<sup>b,c,d,e,\*</sup>, David Schuldberg<sup>f</sup>

<sup>a</sup> Department of Chemistry, University of Montana, Missoula, MT 59812-1584, USA

<sup>b</sup> Complexity Sciences Center, 9225 Collins Avenue, Suite 1208, Surfside, FL 33154, USA

<sup>c</sup> Instituto de Altos Estudos da Paraíba, Rua Silvino Lopes 419-2502, 58039-190 João Pessoa, Brazil

<sup>d</sup> Departamento de Física, Universidade Federal da Paraíba, 58051-970 João Pessoa, Brazil

<sup>e</sup> Institute for Multiscale Simulation, Friedrich-Alexander Universität Erlangen-Nürnberg, D-91052 Erlangen, Germany

<sup>f</sup> Department of Psychology, University of Montana, Missoula, MT 59812-1584, USA

## ARTICLE INFO

## Article history:

Received 22 April 2016

Revised 29 November 2016

Accepted 29 January 2017

Available online 12 February 2017

## Keywords:

Social dynamics

Social models

Psychological stress

Socially buffered response

Stability diagrams

## ABSTRACT

Recent work has introduced social dynamic models of people's stress-related processes, some including amelioration of stress symptoms by support from others. The effects of support may be "direct", depending only on the level of support, or "buffering", depending on the product of the level of support and level of stress. We focus here on the nonlinear buffering term and use a model involving three variables (and 12 control parameters), including stress as perceived by the individual, physical and psychological symptoms, and currently active social support. This model is quantified by a set of three nonlinear differential equations governing its stationary-state stability, temporal evolution (sometimes oscillatory), and how each variable affects the others. Chaos may appear with periodic forcing of an environmental stress parameter. Here we explore this model carefully as the strength and amplitude of this forcing, and an important psychological parameter relating to self-kindling in the stress response, are varied. Three significant observations are made: 1. There exist many complex but orderly regions of periodicity and chaos, 2. there are nested regions of increasing number of peaks per cycle that may cascade to chaos, and 3. there are areas where more than one state, e.g., a period-2 oscillation and chaos, coexist for the same parameters; which one is reached depends on initial conditions.

© 2017 Elsevier B.V. All rights reserved.

## 1. Introduction

Social factors are related to stressful events in many ways. They sometimes generate stressors, are involved in avoiding and appraising them, and contribute to responding and coping with events and their consequences [1]. Since the influential work of Cohen [2], the concepts of social support, stress, and their interaction have been closely tied in both theoretical and empirical work to factors influencing health and well-being. Conversely, stressful events and coping responses are thought to influence the stability of social networks and the availability and maintenance of social supports. A transactional view of stress processes [1] begs for dynamical accounts of how the behavior of these inter-related factors unfolds over time [3–5].

\* Corresponding author.

E-mail addresses: [jason.gallas@cbi.uni-erlangen.de](mailto:jason.gallas@cbi.uni-erlangen.de), [jason.gallas@gmail.com](mailto:jason.gallas@gmail.com) (J.A.C. Gallas).

Social support has been shown to have positive effects on both physical and mental health and potentially to lessen the negative effects of stress. Higher levels of social support are associated with better overall health; the effect is stronger for mental health (such as absence of depressive symptoms) than for physical health. The effects also differ with various kinds of support [6,7]. The so-called stress-buffering hypothesis [8] suggests that in addition to the main effect of amount of support ( $Z$ ) on well-being, social support also has a greater positive effect at higher levels of stress, a moderating process. This buffering is a joint effect of social support and level of stress, e.g., a Perceived Stress ( $X$ ) times Social Support ( $Z$ ) (*vide infra*) interaction.

This stress-buffering hypothesis has led to a good deal of research from which a more nuanced picture has come. The main effects of stress and social support on health are quite well supported [2,6], but the research literature is mixed concerning the existence, magnitude, and even direction of the buffering interaction [7,9]. Nevertheless, the posited interaction of these two factors in relation to an individual's health and well-being, and the research that has followed, have introduced an interesting nonlinear term into this psychological topic [10], with implications when stress and responses to it are looked on as ongoing transactional processes [1] and examined longitudinally over time, both in response to a single stressful event or in the course of multiple stressors or ongoing "complex trauma" [11]. This work examines the dynamic implications of one theoretical form of the nonlinear relationships possibly underlying stress and support-seeking processes.

In a recent work, two of us [5] introduced a dynamic model of stress-related psychological health and illness processes including the nonlinear multiplicative or "buffering" term corresponding to the interaction discussed in the stress-buffering hypothesis [2,8]. This dynamical model of stress consists of three nonlinear differential equations describing varying states of a person, perceived stress ( $X$ ), symptoms of physical and psychological ill-health ( $Y$ ), and social support ( $Z$ ). This model was used to simulate the behavior of an individual under stress, the stationary-state stability properties of this behavior, its temporal evolution, as well as how each variable affects the others. The current paper extends this previous work and explores the role of periodic fluctuations in environmental stress on the behavior of the model, investigating the control space associated with this forcing variable. While the primary interest of this paper is exploring these theoretical dynamics mathematically, it also connects model behavior with possible corresponding psychological constructs.

## 2. Dynamic models of stress processes

What is presently known about nonlinear dynamic models of stress? Considering that time may be modeled as either discrete or continuous, it is possible to study temporal unfolding of aspects of the stress response in several ways. First, discrete-time models utilize iterative processes where a suitable function maps the state of the system at  $t_n$  to its state at  $t_{n+1}$ . For example, in the systems models of Smith and Stevens [4], each variable's predictive function is given by levels of variables (including itself) multiplied by appropriate weights, similar to the simple logistic mapping in population dynamics [12]. These authors provide an iterative model of two-person psychological attachment and comfort, including something like social support in the "soothing" of one person via an attachment relationship with another. Their six equations contain nonlinear (product, reciprocal, and squared reciprocal) terms. One of us [13] adapted a dynamic model of stress and support-seeking from another iterative model, the delayed logistic map [14]. This contained a multiplicative (Stressor  $\times$  Social support) term and used "experienced stress" to index ill-health. Continuous-time ordinary differential equations have also been used to study stress, notably by Neufeld [3], as well as to explore marital interaction [15], romantic love, and courting [16,17, 18]. Neufeld's dynamic stress model contains six variables: stressors (what we are calling Perceived stress), cognitive efficiency, decisional control, stress-sensitivity, and coping sensitivity. While not focusing on social-support per se, the model does have some constructs that overlap with this paper's and includes multiplicative terms. Also noteworthy is work on discontinuities and catastrophe dynamics relevant to stress and illness [19]; a number of different catastrophes can be modeled across two points in time, time series, and the continuous time of the underlying model [20,21,22].

## 3. Our socially buffered response model

According to Field and Schulberg's approach [5], stressor levels and social-support variables are taken to influence the rate of change of each other. It is assumed that the overall rate of change of one variable may be written as a sum of contributions by various distinct causal paths expressed as suitable multiplicative terms of the form *variables*  $\times$  *weights*. Thus, the model considered here is [5]:

$$\frac{dX}{dt} = k_1A + (k_2B - k_6)X + k_3Y - k_4XZ - k_5X^2, \quad (1)$$

$$\frac{dY}{dt} = k_6X - k_7Y, \quad (2)$$

$$\frac{dZ}{dt} = k_8(S_0 - Z)Y - \beta k_4XZ - k_9Z. \quad (3)$$

It involves three dynamic dimensionless variables  $\{X(t), Y(t), Z(t)\}$ , describing the state of the system at a particular time  $t$  and for a particular set of model parameters: (a)  $X(t)$  = Perceived psychological stress experienced by an individual, which

**Table 1**  
Parameter values used in our simulations.

Parameter	$A_0$	$S_0$	$\beta$	$k_3$	$k_4$	$k_5$	$k_6$	$k_7$	$k_8$	$k_9$
Value	1	10	0.5	0.01	2	0.3	0.01	0.01	0.1	0.01

**Table 2**  
Quantifiers of the temporal evolution of the oscillations of  $X$ ,  $Y$ ,  $Z$  for  $\rho = 1$ , shown in Fig. 4. The six values of  $\omega$  are indicated in Fig. 3. Here,  $p_x, p_y, p_z$  refer to the number of spikes in  $X, Y, Z$  oscillations, respectively, while  $\lambda_2, \lambda_3$  are the two non-zero Lyapunov exponents. Note the non-uniform variation of both periods and exponents.

$\omega$	$p_x$	$p_y$	$p_z$	Period	$\lambda_2$	$\lambda_3$
0.16	3	1	3	117.81	-0.06129	-0.40931
0.21	4	1	4	119.68	-0.09637	-0.39090
0.27	5	1	5	116.36	-0.04874	-0.39221
0.32	7	1	7	137.44	-0.03476	-0.42610
0.36	8	1	8	139.62	-0.02625	-0.42929
0.45	11	1	11	153.59	-0.03366	-0.39071

can be measured by self-reported or observed stressors, hassles [23], or potentially traumatic or taxing life events. This is perceived stress because it includes such factors as the person’s cognitive appraisal [1] of an event. (b)  $Y(t)$  = Symptoms of stress-related ill-health experienced by this individual. Serving as a proxy for physical or psychological symptoms, it can be measured by a variety of clinical instruments. And, (c)  $Z(t)$  = Social support received, diminishing  $X$  by way of the “buffer”  $-k_4XZ$  term in the  $dX/dt$  equation;  $Z$  can be measured as tangible and emotional assistance received, number of involved friends and family members, or in other ways. It is assumed that only limited social support is available. Thus  $S_0 = U + Z$ , where  $S_0$  is total available social support,  $Z$  is the amount of social support currently in use, and  $U$  is the amount of social support that is available but currently not involved in ameliorating or buffering stress.

In Eqs. (1)–(3), the rate parameters  $k_i$  are related to the personality of the individual under stress;  $A$  and  $B$  are two theoretical and experimentally defined measures of environmental stress. All weights are treated as expendable parameters, but fitting model results to empirical observation would allow estimating them for a particular individual and environment for testing the fit of this or a similar model to psychological data. Table 1 gives the parameter values typically (and initially) used in the simulations.

Eq. (1) contains six polynomial terms (resulting from six interactions involving the variables,  $X, Y$ , and  $Z$ ) that contribute to the rate of change of  $X, dX/dt$ . The rates of the six interactions are assumed proportional via the appropriate values of  $k_i$  to the instantaneous levels of the interacting quantities  $X, Y, Z$ . In Eq. (1),  $A$  and  $B$  refer to two types of different environmental or ambient stressors, each responded to differently:  $A$  refers to ambient events and circumstances that directly raise the stress response, and  $B$  to events where the growth of stress occurs as a result of stress itself.

It is the  $B$  parameter that is primarily varied below in analyses of the dynamic properties of this model. We believe that this auto-catalytic form of stressor and the person’s sensitivity to it are particularly important psychologically and physiologically under both healthy and pathological conditions. This is a parameter that to a large extent controls the stability of the model.

In the discussions that follow we describe the model, as well as psychological processes potentially corresponding to parameters and terms in the equations. Then the paper explores dynamics in the behavior of the model and describes some observed trajectories and patterns, particularly as certain crucial parameters are varied.

Beginning with describing terms and parameters, the  $+k_1A$  term is the contribution of the first (non-catalyzing) kind of Environmental stress,  $A$ , to  $dX/dt$ . Here,  $k_1$ , fixed to  $k_1 = 1$ , reflects sensitivity to growth of  $X$  at a particular level of stress,  $A$ . For example, potentially traumatic environmental events generally increase perceived stress (via the  $A$  term). The  $+k_2B$  term reflects the above-mentioned self-catalyzed growth in  $X$  in response to stress itself. Perceived stress may generate more stress, with the strength of this feedback depending on  $k_2$ . Some situations (such as an event for which a person feels responsible) can amplify the effects of the current level of perceived stress, perhaps via the emotions of guilt or shame [24]. Higher levels of Perceived stress can also lead to some behaviors that have a negative effect, such as angry or inefficient efforts at coping or excessive reassurance seeking [25,26], efforts that can backfire. This term considerably increases the model’s dynamic richness. In the numerical work reported here, the  $A$  component of stress is included in the periodic forcing equation found to provoke chaotic behavior. The parameter  $B$  is also varied in studying the dynamic behavior of the model.

The  $+k_3Y$  term reflects increasing perceived stress resulting from increasing symptoms,  $Y$ . For example, increasing alcohol consumption, a symptom component of  $Y$ , might result in more Perceived stress,  $X$ , not less. Here we fix  $k_2 = 1$ . The  $-k_4XZ$  term is the buffering effect of the - Stress  $\times$  Social support interaction. The  $-k_5X^2$  contribution reflects higher-order loss processes appearing when the level of Perceived stress becomes very high; it might be related to acute or emergency

medical attention or other factors limiting the amount of adversity one can experience. An additional  $-k_i X$  term could be added to describe efforts by the individual to counteract or ameliorate the effects of environmental stressors, for example *problem-focused coping* [1], or to account for the fact that subjective distress is likely to have an upper bound. This term does not significantly change the dynamics and its effect is included in the value of  $k_6$ .

In Eq. (2), the Stress term  $+k_6 X$  causes growth of Symptoms,  $Y$ ; this is the primary mechanism of the well-established effect of stress on psychological symptoms. In contrast, the  $-k_7 Y$  term refers to decreasing symptoms via routes other than use of social support, e.g., through fatigue, non-acute intervention, or self-limiting processes. The complementary  $-k_6 X$  term appearing in the  $dX/dt$  (Stress) equation was originally added as a mass balance [27] term. However, it does actually seem to correspond to the longstanding clinical observation [28] that expression of symptoms can decrease stress (e.g., resulting from *psychological conflict*). Other mass-balance terms considered were found not psychologically sensible and dropped.

In Eq. (3), the  $+k_8 Y(S_0 - Z)$  term arises where  $Y$  (Symptoms) convert uninvolved social support,  $U$ , to involved,  $Z$ . The  $-(\beta k_4) XZ$  is also a form of mass balance. Each time a buffering event ( $-k_4 XZ$ ) occurs,  $Z$  diminishes as it is only partially converted to  $U$ . The  $0 < \beta \leq 1$  multiplier causes conversion of  $Z$  to  $U$  to occur in only a fraction of buffering events. This term captures a social-support fatigue effect, “compassion fatigue” [29], or temporary “burnout” of supportive others, or – in extreme situations – when others around the person may start to experience “Secondary Traumatic Stress” [30]. The  $-k_9 Z$  term is a decay term for  $Z$  suggesting that providing support slowly self-decays to  $U$ , regardless of the support-seeker’s symptom state  $Y$ .

The model above is similar (but not identical) to the very successful Oregonator model [31] of the oscillatory Belousov–Zhabotinsky (BZ) chemical reaction [32]. Such models are versatile and, with suitable parameter values, yield psychologically reasonable results that exhibit the entire gamut of nonlinear dynamical behavior, e.g., oscillation, spatial pattern formation, multiple stationary states, bursting, and chaos [33,34]. For most parameter values, though,  $X(t)$ ,  $Y(t)$ , and  $Z(t)$  simply approach unchanging (but dynamic) stationary states with constant levels of  $X(\infty)$ ,  $Y(\infty)$ , and  $Z(\infty)$ . These stable stationary states correspond to diverse “everyday” and “normal” dynamics of individuals’ regulated functioning with regard to stress and symptoms of illness and inform contemporary interpretations of homeostasis [5].

Now that the causal connections and processes in the models have been elucidated and described in psychological terms, the next tasks are to probe the dynamics and patterning of the model’s behavior and attempt to frame these characteristics of dynamics in similar psychological language. A parameter search conducted by Field and Schulberg [5] revealed that Eqs. (1)–(3) do not seem to support chaotic oscillations in stress level and support seeking. However, chaotic variations were found for several situations under periodic stressor modulation of the environmental stress value  $A$  of the form

$$A = A_0 + \rho \sin(\omega t), \quad (4)$$

where  $\rho$  and  $\omega$  are the amplitude and angular frequency of the modulation, respectively.

Here, we present a systematic investigation of the periodic forcing on the distribution of regular and chaotic changes in stress response predicted by the stress model as a function of some of the main parameters controlling stress levels. These three psychological factors are  $B$ , corresponding to stressors that evoke self-acceleration, and the frequency-amplitude parameters  $\omega \times \rho$  of periodic environmental modulation of one form of stressor on an individual. The frequency and magnitude of environmental stressors are two parameters with great effects on the stability of the system; as  $\omega$  or  $\rho$  is increased, the person experiences more rapid and larger incidence of stressors or potentially traumatic life events. High levels correspond to “complex trauma” [11], possibly over an extended period of time. Such situations are involved in proposed new diagnostic categories, Complex trauma disorder and Developmental Trauma Disorder in children [35] and Post-Traumatic Stress Disorder in combat participants. Investigating  $\omega$  and  $\rho$  captures both intensity and the rapidity of ongoing exposure.

#### 4. Predicted distribution of stress variations for our socially buffered response model

The first and third rows of Fig. 1 present a sequence of frequency ( $\omega$ ) vs. amplitude ( $\rho$ ) stability diagrams illustrating how the complex oscillations of  $X$  evolve from  $B = 0.6$  up to  $B = 3.22$ . Below each stability diagram, Fig. 1 presents bifurcation diagrams displaying the maxima of  $X$  vs.  $\omega$  along the white line at  $\rho = 10$ , a level of stressor intensity where many of the relevant dynamic phenomena occur in this system as seen in the stability diagrams. The diagrams were computed and plotted as described in Methods. The colorbar on the bottom row of Fig. 1 indicates the code used to define parameter regions characterized by periodic oscillations having the same number of spikes per period. As indicated for  $B = 0.6$  (leftmost panel on the top row), frequencies and amplitudes leading to 1-spike oscillations are shown in blue, 2-spikes in green, and for  $B \geq 1$  oscillations with 4-spikes are in red. Black pixels here and elsewhere represent chaotic behavior for a particular set of parameters, namely oscillations with no numerically detectable periodicity. As seen from the bifurcation diagram for  $B = 0.6$ , the wide 1-spike blue phase seems to be divided into two sub-phases: on the left one finds 1-spike oscillations with amplitudes larger than those observed in the other sub-phase, on right of the 2-spikes green phase. At higher frequencies of instances of self-accelerating stressful events, the rightmost panels on the top row reveal that a new phase characterized by complex alternation of periodic oscillations emerges from the bottom. Simultaneously, the 2-spikes phase undergoes a peak-doubling cascade with phases of chaos, 3-spikes, etc. appearing in its inner part. The bifurcation diagrams also show that the subdivision into regions of larger and smaller amplitude oscillations persists. As illustrated by the stability diagrams on the third row, a regular series of striations dominates the lower part of the diagram near  $\rho = 0.5$  to 1. As  $B$  is further increased, the new phase breaks into two disconnected pieces and quickly shrinks. The regions of periodic oscillations may be thought

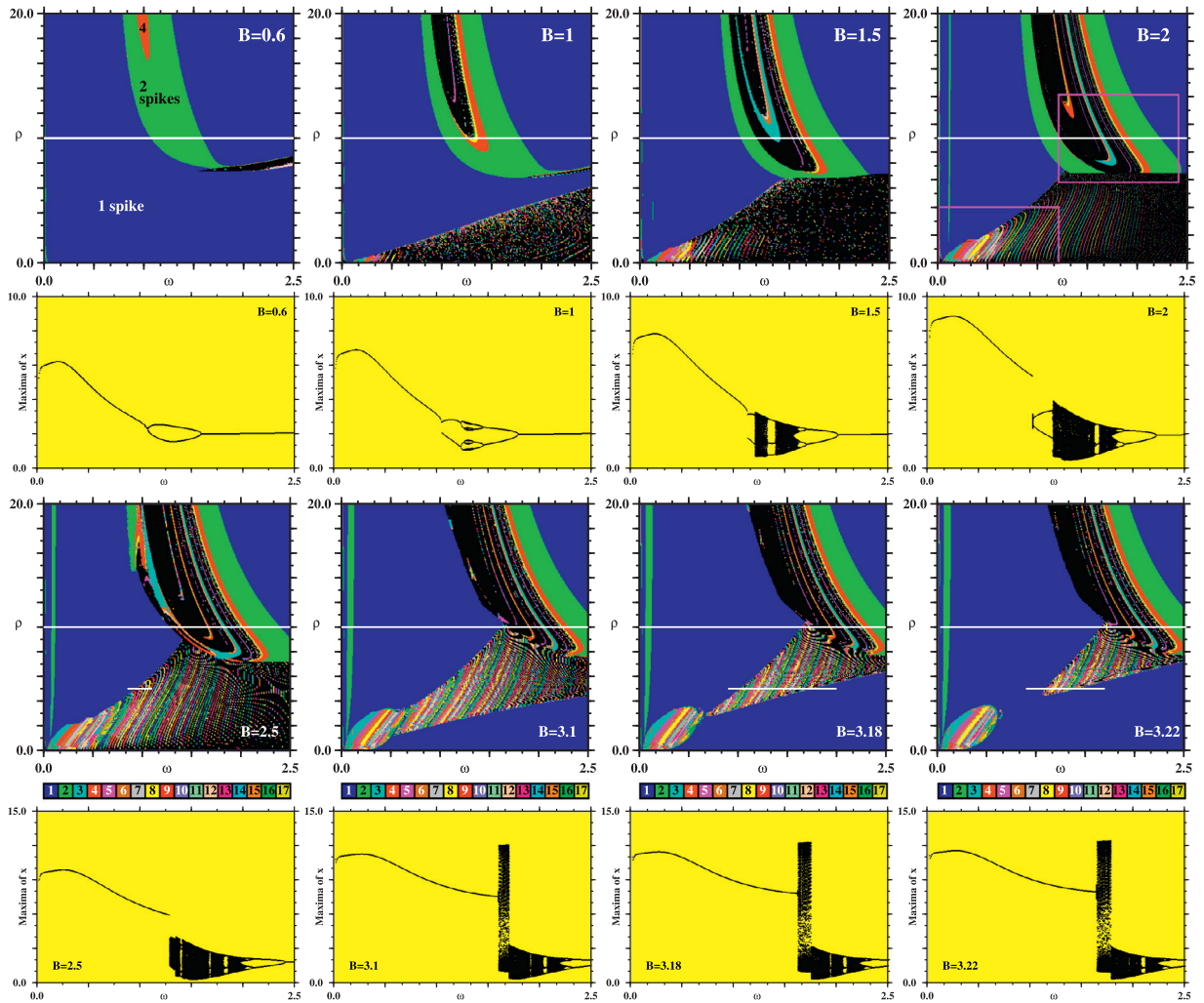


**Fig. 1.** Evolution of the frequency-amplitude stability diagram in  $\omega \times \rho$  space as a function of  $B$ , a measure of sensitivity to autocatalytic stress growth in an individual that is separate from  $A$ , ambient stress. On the third row, the small white segments for  $\rho = 5$  on panels for  $B = 2.5, 3.18,$  and  $3.22$  mark the intervals of  $\omega$  depicted on the bifurcation diagrams in Fig. 2. The two boxes seen on the panel for  $B = 2$  are magnified in Fig. 3. Colors reflect the number of spikes per period of  $X$ .

of as corresponding to quasi-homeostatic regulated behavior without much deviation from some sort of baseline or set-point behavior. However, at high levels of the auto-catalysis-related form of stressor,  $B$ , as well as repeated high-amplitude environmental events, more complex behavior occurs.

Fig. 2 shows three additional bifurcation diagrams computed for  $X, Y,$  and  $Z$  to understand the nature of the complex alternation of oscillations composing the colorful stripes. Such diagrams are computed along the white line segments drawn along  $\rho = 5$ , for the panels  $B = 2.5, 3.18,$  and  $3.22$  on the third row of Fig. 1. The diagrams illustrate the complex alternation of chaos and periodicity for these parameters. They also show that the amplitude of  $X$  (Perceived stress) is essentially independent of  $\omega$  (the frequency of stressors) over relatively large intervals. Thus, even when stressful events are occurring at a high frequency, the behavior of this model shows quite bounded levels of perceived stress. From a psychological point of view, it is interesting that despite the observed alternations between chaos and periodicity, the magnitude of perceived stress tends to stay within broad bounds. This also speaks to how a variety of “strategies,” mechanisms, or behavioral regimes can maintain some sort of bounded, if not steady or stationary, state.

In Fig. 2, at both lower and very high levels of the self-kindling stressor parameter, behavior is oscillating but somewhat periodic and regular. However, in the middle panel of Fig. 2, chaotic behavior begins, perhaps corresponding to circumstances where a person’s stress response, coping and recruitment of social support, while functional and remaining bounded, are unpredictable and sensitive to the relatively small vagaries of changes in psychological or environmental variables.

Fig. 1 illustrates stability diagrams obtained by counting spikes in the  $X$  variable. What do stability diagrams look like for the other two variables,  $Y$  and  $Z$  (symptoms and levels of social support)? The answer is given in Fig. 3 where the panels

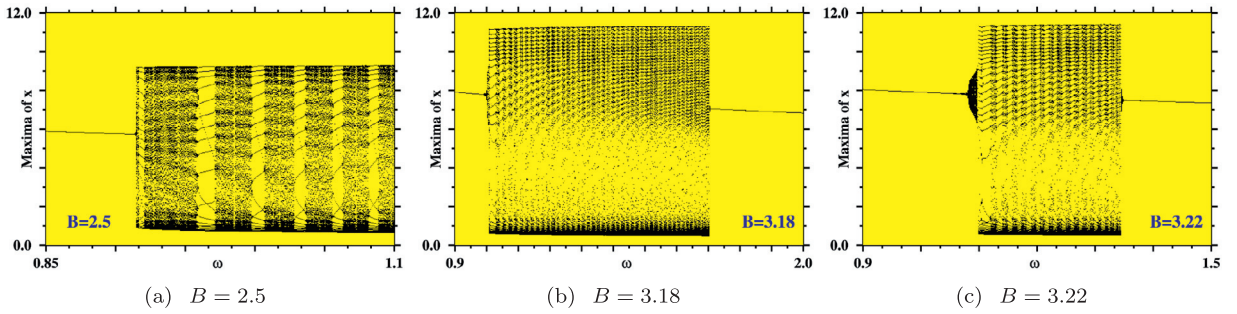


**Fig. 2.** Bifurcation diagrams illustrating alternation of chaos and periodic oscillations with many spikes per period. These diagrams are computed for  $\rho = 5$ , along the white segments indicated on the third row of Fig. 1, in the panels for  $B = 2.5, 3.18$ , and  $3.22$ .

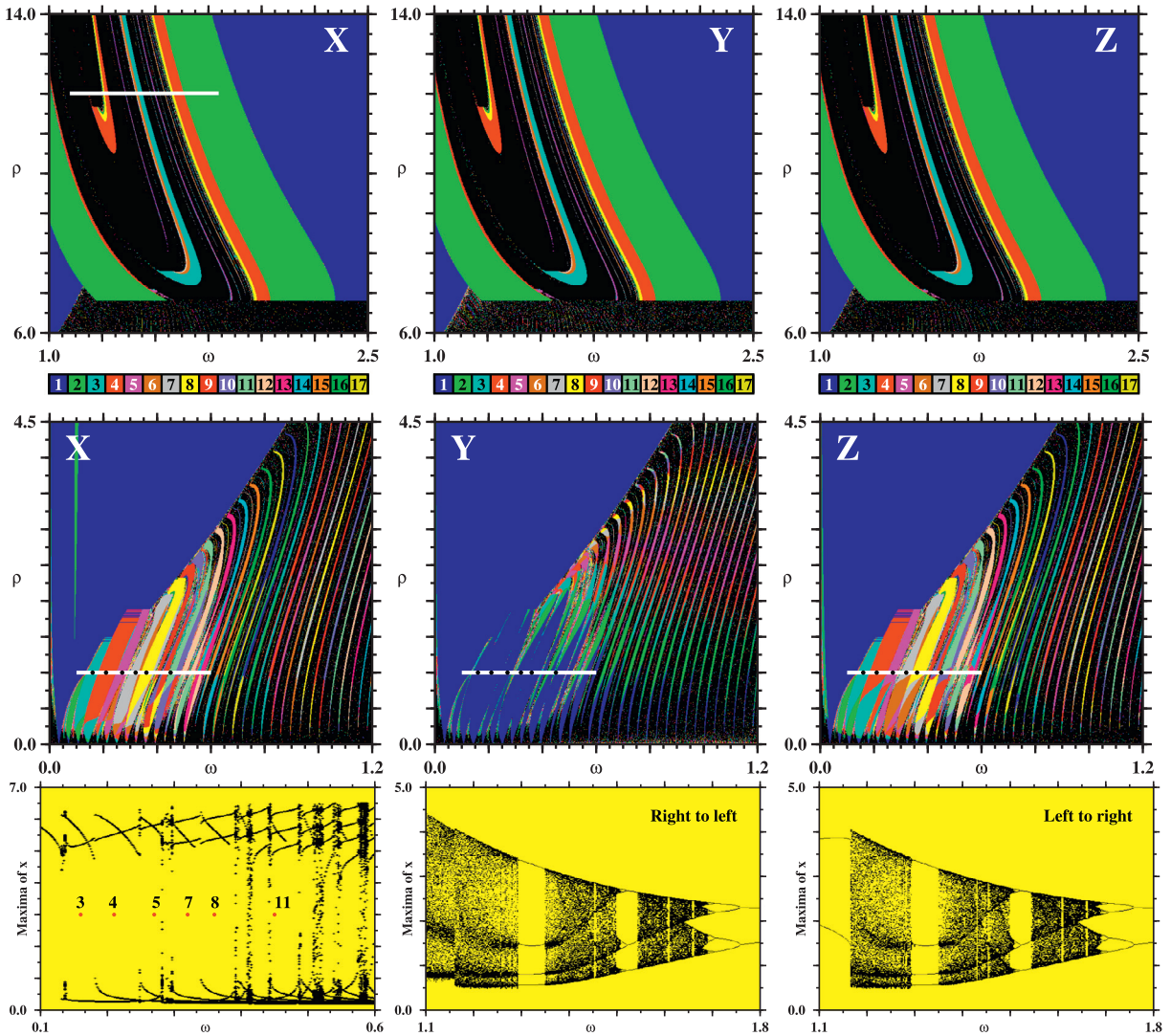


**Fig. 3.** Complex stability regions recorded on the frequency ( $\omega$ ) vs. amplitude ( $\rho$ ) control plane. The top and center rows show magnified views of the boxes marked in the upper right panel for  $B = 2$  in Fig. 1. In each row, panels show stability diagrams obtained by counting the number of spikes per period of  $X, Y, Z$ , as indicated. In the bottom row, the leftmost panel shows a bifurcation diagram computed along the white segment  $\rho = 1$  indicated on the three panels in the middle row. To facilitate comparison, the six points seen on the leftmost panel of the middle row are superposed on the leftmost bifurcation diagram on the bottom row. Numbers refer to the number of spikes of the oscillations. Coordinates and other relevant data for these points are listed in Table 2 (see text). The two other bifurcation diagrams display the existence of multistability and hysteresis in the system. Both diagrams are calculated along the white horizontal line  $\rho = 12$  seen on the leftmost panel on the top row. Here  $B = 2$ . Individual panels display the analysis of  $1200 \times 1200$  parameter points.

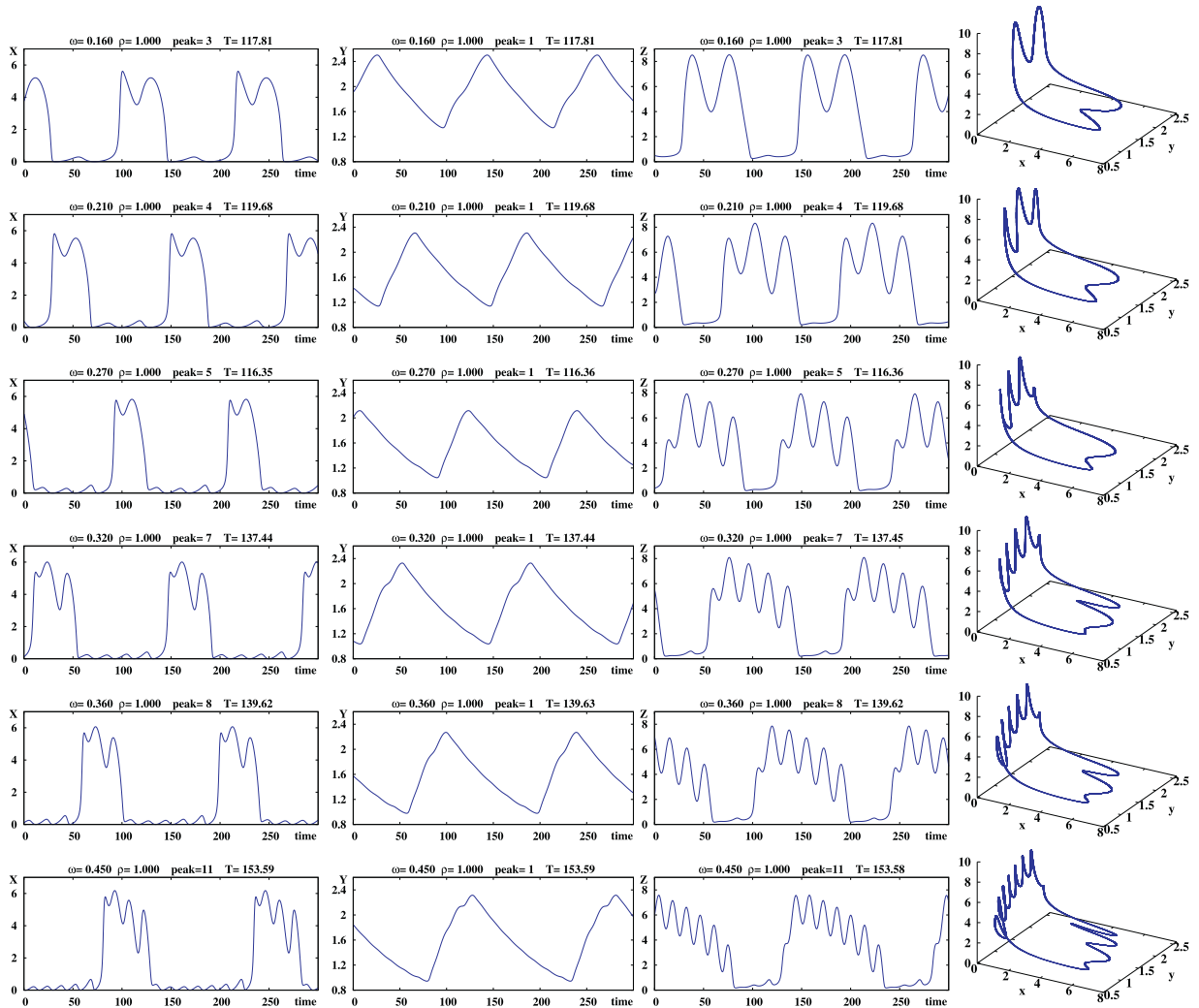


**Fig. 4.** Temporal evolutions of  $X, Y, Z$  computed for the six points indicated in Fig. 3. These evolutions agree with the characterizations for the six points along the horizontal line at  $\rho = 1$  seen in the middle row of Fig. 3. Note the very subtle distortions of small amplitude in the oscillations of  $Y$ . The variable  $Z$  contains peaks that are too small to be discernible on this scale. The precision of the period  $T$  is  $\pm 0.01$  (arbitrary units) and is fixed by the step of the numerical integrations. Here  $B = 2, \rho = 1$ .

in the first two rows show magnified views of the two pink boxes marked in the third row of Fig. 1. Although they display roughly the same structure, specific details in each diagram depend on the dynamical variable considered. The bottom row in Fig. 3 shows bifurcation diagrams computed along the white segments indicated on both  $X$  panels. The several branches seen on these diagrams display the loci of the local maxima (spikes) of the  $X$  variable. To facilitate comparison, the six points seen on the center panel are superposed on the leftmost bifurcation diagram. This diagram reveals a rather complex sequence of periodic oscillations whose precise organization remains an open problem. Again note that bounded behavior is maintained. The two rightmost bifurcation diagrams on the bottom row provide evidence of multistability: they were computed by scanning the white line from right to left and from left to right as indicated, always starting from the same fixed initial condition and following the attractor (see Methods). The difference between this pair of diagrams is evidence of a hysteresis phenomenon in this region. The succession of stripes seen in the middle row of Fig. 3 resembles the organization observed recently on a rather distinct context, namely in an enzyme reaction model [36].

To understand the origin of the differences between the separate stability diagrams obtained by counting spikes of  $X, Y, Z$ , we investigated how the waveforms of these variables change for the six points along  $\rho = 1$ , as indicated in the middle  $X$  (Perceived Stress) panel in Fig. 3. Such temporal evolutions are illustrated in Fig. 4. From this figure it is clear that the spikes are much more pronounced in  $X$  (Perceived Stress) and  $Z$  (Social Support received), with  $Y$  (level of clinical Symptomatology) presenting smooth and relatively mild distortions. The oscillations in symptoms appear as a series of sawteeth, with little internal structure. In contrast, when the oscillations in  $Z$  (Social Support) reach a high level, there are more dynamics, with small oscillations on top of the larger ones; this explains the origin of the differences between the stability diagrams of

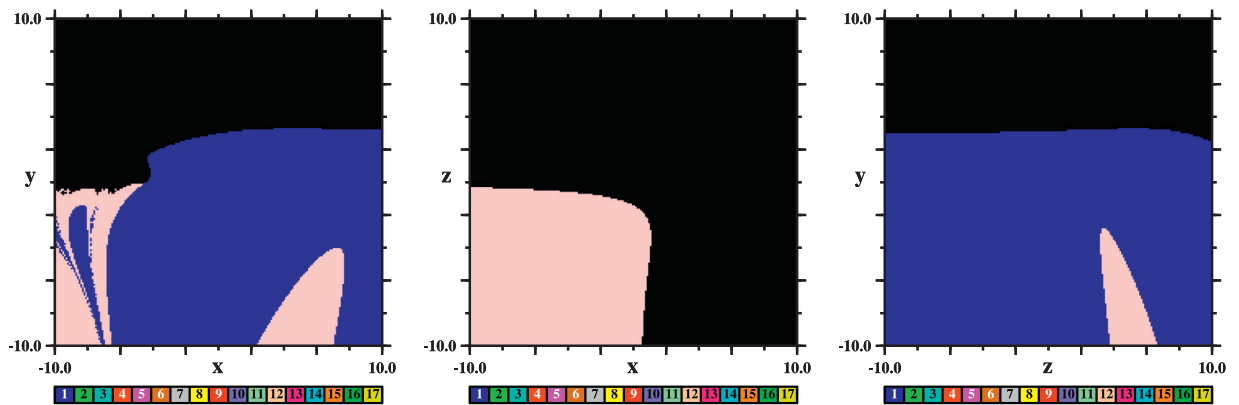


**Fig. 5.** Three basins of attraction illustrating multistability in the phase space of the system. Basins are centered around the (arbitrary) initial condition  $(X_0, Y_0, Z_0) = (0.1, 0.1, 5.19)$ . The color coding is defined by the number of spikes of  $X$ . Black denotes values leading to chaotic oscillations, blue to 1-spike oscillations, and pink to divergent solutions. The diagrams include negative values of the variables, which have no meaning for the application considered here. (For interpretation of the references to colour in this figure legend, the reader is referred to the web version of this article.)

**Fig. 3.** The variable  $Z$  also presents spikes that are greater by an order of magnitude in their amplitude. The same is true (to a lesser extent) with Perceived Stress. In the third column of the last row of **Fig. 4** we see a structure of decreasing (damped) levels of support, followed by a large drop to a low state. The successfully moderated low-stress state appears more dynamic than the high stress state, where the stress response appears to be fighting to keep stress in check. We suggest these damped oscillations in  $Z$  result as support moves back-and-forth between the involved and uninvolved pools until nearly the entire pool of supporters is eventually fatigued.

The well buffered (low) stable state is still dynamic, with small, perhaps slightly increasing oscillations. The different pictures for Stress and Support on the one hand and Symptoms on the other explain the origin of the differences between the stability diagrams in the center row of **Fig. 3**. The Social support variable  $Z$  also presents spikes that are greater by an order of magnitude in their amplitude. A potential interpretation of this is that Stress and Social support show bistability, while symptoms simply become a series of sawteeth. We also see here somewhat intricate inter-variable variations, much more complicated than would be predicted by an equation with two main effects and a multiplicative term across various instants. The phase diagrams in the right-hand column show the interrelationships among these variables at particular points in the parameter space and the resultant overall dynamics of the system.

**Fig. 5** again illustrates the presence of multistability in the model. Depending of the initial conditions the dynamics may converge asymptotically either to a 1-spike oscillation, to a chaotic oscillation, or simply diverge. Multi-stability is abundant in the system and would require a huge amount of computation to be precisely delimited in stability diagrams. The multi-stability is interesting from a psychological point of view. In these regions of different attractors the person and potentially supportive others can fall or be pushed into one or the other of these regimes.

With periodic forcing a variety of interesting stress dynamics result. Moreover, at high levels of  $B$ , the important role emerges for the type of stressor that promotes self-kindling, chaos, rapid transitions between dynamic regimes, and multi-stability. In addition, **Fig. 5** illustrates that there are areas where the variables diverge, apparently corresponding to reactions in very extreme circumstances, including psychological decompensation, exhaustion, and collapse [37]. Such diverging represents a “runaway process” where, in spite of the down-regulating processes built into the model, the system runs out of control. Particularly in the face of stressors promoting self-catalyzing, people may decompensate in complex, diverse, and rapidly changing ways. Difficult situations may be more complicated if they are oscillating. This seems in accord with some of our psychological intuitions and observations.

## 5. Conclusions and outlook

The main thing that we can say psychologically is that this model is a very fundamental dynamic system of a form that seems to appear in many physical and biological scenarios. Its major feature is an autocatalytic process moderated by a negative feedback loop. The major suggestion of our calculations is that under periodically perturbed stress an individual’s behavior may become unstable and pass through many complex behaviors, including chaotic states where behavior may become unpredictable.

In the case of a chemical system, the governing dynamic equations must reflect the underlying conservation of mass, defined by the so-called stoichiometry [27] of the overall chemical reaction. We know relatively little about the psychological, interpersonal, and biological stoichiometry of human interactions, but a “stoichiometric” analogy might carry over from chemistry to psychology. We added appropriate mass-balance terms to **Eqs. (1)–(3)**. We believe this approach holds promise for describing coupled mechanisms in psychological adaptation and self-regulation, as well as “ironic” [38] and even “spontaneous” behavior. There are regions where the model’s qualitative dynamics appear analogous to successful

coping, homeostasis in the stress response, as well as behavior corresponding to psychological and social crisis or being overwhelmed. Importantly, the role and implications of multiplicative terms in stress and coping are different when our models become dynamic ones. And, we see no recognizable behavioral sign of the buffering effect (modeled by a simple multiplicative term) posited in the stress buffering hypothesis. Will a multiplicative term in a cross-sectional predictive equation or a theoretically-based model in the social support buffering literature imply underlying generating equations containing the same multiplicative terms? In this case, apparently not: the buffering term in these differential equation does not result in a  $-XZ$  relationship in the overall dynamic structure of the model [5], at least as far as we can tell.

The methods developed in this paper can be extended to other continuous nonlinear dynamic models of adaptation, adjustment, coping, and recovery from setback. An ongoing question concerns the extent to which the relationships found in single-point-in-time cross-sectional psychological research on psychological processes may or may not provide insights into these same processes' underlying dynamics.

## Acknowledgements

JACG was supported by CNPq, Brazil. This work was supported by the Deutsche Forschungsgemeinschaft (DFG) through the Cluster of Excellence *Engineering of Advanced Materials*. The authors acknowledge use of the CESUP-UFRGS clusters located in Porto Alegre, Brazil.

## Appendix

The isospike diagrams [39–41] in Figs. 1, 3, and Fig. 5 were obtained by solving the model equations numerically; the parameter values are those in Table 1, unless indicated otherwise. We used the standard fourth-order Runge-Kutta algorithm with fixed-step,  $h = 0.01$ , over a mesh of equally spaced points, usually  $1200 \times 1200$  points. For each value of  $\omega$ , integrations were started from the arbitrary initial condition  $(X, Y, Z, t_0) = (0.1, 0.1, 5.19, 5.1)$  and continued mostly from left to right by following the attractor [42–44], namely by using the last obtained values of the variables to start every new integration involving infinitesimal changes of parameters. The first  $10^6$  time-steps were discarded as transient time needed to reach the final attractor. The subsequent  $10^6$  iterations were then used to compute the number of spikes contained in one period of the oscillations, by recording up to 800 extrema (maxima and minima) of the time series of the variable under consideration, together with the instant when they occur, and recording repetitions of the maxima. As indicated by the colorbar in the figures, a palette of 17 arbitrary colors was used to represent “modulo17” (i.e. recycling colors) the number of peaks (maxima) contained in one period of the oscillations. The bifurcation diagrams in Figs. 1, 2, and 3 were obtained by the same procedure described above, plotting the local maximum values (spikes) of the variable of interest. In such diagrams, both axes were divided into 600 equally spaced values. For additional details concerning the computation of stability diagrams see the survey in Ref. [44].

## References

- [1] Lazarus RS, Folkman S. Stress, appraisal, and coping. New York: Springer; 1984.
- [2] Cohen S. Stress, social support, and disorder. In: Veiel H, Baumann U, editors. The meaning and measurement of social support; 1992. p. 109–24. New York: Hemisphere Press.
- [3] Neufeld RWJ. Dynamic differentials of stress and coping. Psychol Rev 1999;106:385–97.
- [4] Smith T, Stevens GT. Biological foundations of social interaction: Computational explorations of nonlinear dynamics in arousal modulation. In: Eve R, Horsfall S, Lee M, editors. Chaos, complexity, and sociology: myths, models, and theories; 1997. p. 197–214. Thousand Oaks CA: Sage.
- [5] Field RJ, Schuldberg D. Social-support moderated stress: a nonlinear dynamical model and the stress-buffering hypothesis. Nonlin Dyn Psychol Life Sci 2011;15:53–85.
- [6] Ganster DC, Victor B. The impact of social support on mental and physical health. British J Med Psychol, Special Issue 1988;61:17–36.
- [7] Procidano ME. The nature of perceived social support: findings of meta-analytic studies. Adv Person Assess 1992;9:1–26.
- [8] Cohen S, Wills TA. Stress, social support, and the buffering hypothesis. Psychol Bull 1985;98:310–57.
- [9] Alloway R, Bebbington P. The buffer theory of social support: a review of the literature. Psychol Med 1987;17:91–108.
- [10] Carver CS, Scheier MF. On the self-regulation of behavior. New York: Cambridge University Press; 1998.
- [11] Cohen JA, Mannarino AP, Kliethermes M, Murray LA. Trauma-focused CBT for youth with complex trauma. Child Abuse Negl 2012;36(6):528–41.
- [12] May RM. Theoretical ecology: principles and applications. 2nd edition. Oxford: Blackwell; 1981.
- [13] Schuldberg D. Complicato ma non troppo: a small nonlinear model and the good life. In: Delle Fave A, editor. Dimensions of well-being: research and intervention; 2006. p. 552–6. Milan: Franco Angeli.
- [14] Aronson DG, Hall MA, McGehee RP. Bifurcations from an invariant circle for two-parameter families of maps of the plane: a computer-assisted study. Commun Math Phys 1982;83:3033–354.
- [15] Gottman JM, Swanson JD, Tyson CC, Swanson KR. The mathematics of marriage: dynamic nonlinear models. Cambridge: MIT Press; 2002.
- [16] Strogatz S. Nonlinear dynamics and chaos with applications to physics, biology, chemistry, and engineering. 2nd edition. Boulder; Westview Press; 2015.
- [17] Sprott J. Dynamical models of love. Nonlin Dyn Psychol Life Sci 2004;8:303–14.
- [18] Rinaldi S, Rossa FD, Dercole F. Love and appeal in standard couples. Int J Bif Chaos 2010;20:2443–51.
- [19] Guastello SJ. Accidents and stress-related health disorders: forecasting with catastrophe theory. In: Quick J, Hurrell J, Murphy L, editors. Work and well-being: assessments and interventions for occupational mental health; 1992. p. 252–69. Washington, DC: American Psychological Association.
- [20] Guastello SJ. Chaos, catastrophe, and human affairs: applications of nonlinear dynamics to work, organizations, and evolution. Mahwah, New Jersey: Lawrence Erlbaum Associate Publishers; 1995.
- [21] Guastello SJ. Catastrophe models with nonlinear regression. In: Guastello S, Gregson R, editors. Nonlinear dynamical systems analysis for the behavioral sciences using real data. New York: CRC Press; 2011a. p. 305–18.
- [22] Guastello SJ. Discontinuities and catastrophes with polynomial regression. In: Guastello S, Gregson R, editors. Nonlinear dynamical systems analysis for the behavioral sciences using real data; 2011b. p. 231–80. New York: CRC Press.

- [23] DeLongis A, Coyne JC, Dakoff G, Folkman S, Lazarus RS. Relationship of daily hassles, uplifts, and major life events to health status. *Health Psychol* 1982;1:119–36.
- [24] Dewey D, Schuldberg D. Criterion a, peritraumatic emotions, and posttraumatic stress disorder. *Traumatology (Tallahass Fla)* 2013;X:1–16.
- [25] Joiner TE, Alfano MS, Metalsky G. When depression breeds contempt: reassurance seeking, self-esteem, and rejection of depressed college students by their roommates. *J Abnorm Psychol* 1992;101:165–73.
- [26] Starr LR, Davila J. Excessive reassurance seeking, depression, and interpersonal rejection: a meta-analytic review. *J Abnorm Psychol* 2008;117:762–75.
- [27] Field RJ. Chemical kinetics. *Scholarpedia* 2008;3:4051.
- [28] Breuer J, Freud S. *Studies on hysteria*, translated by strachey j.. New York: Basic Books; 2000.
- [29] Figley CR. *Treating compassion fatigue*. New York: Routledge; 2002.
- [30] Borntreger C, Caringi JC, van den PR, Crosby L, O'Connell K, Trautman A, et al. Secondary traumatic stress in school personnel. *Adv Sch Ment Health Promot* 2012;5(1):38–50.
- [31] Field RJ, Noyes RM. Limit cycle behavior in a model of a real chemical reaction. *J Chem Phys* 1974;60:1877–84.
- [32] Field RJ, Körös E, Noyes RM. Oscillation in chemical system. II thorough analysis of temporal oscillation in the bromate-cerium-malonic acid system. *J Am Chem Soc* 1972;94:8649–64.
- [33] Epstein IR, Pojman JA. *An introduction to nonlinear chemical dynamics*. New York: Oxford University Press; 1998.
- [34] Scott SK. *Chemical chaos*. Oxford: Clarendon; 1991.
- [35] Ake GS, Ko SJ, Gerrity ET, Steinberg AM, Howard ML, Pynoos RS, et al. Complex trauma and mental health in children and adolescents placed in foster care: findings from the national child traumatic stress network. *Child Welfare* 2011;90(6).
- [36] Gallas MR, Gallas JAC. Nested arithmetic progressions of oscillatory phases in Olsen's enzyme reaction model. *Chaos* 2015;25:064603.
- [37] Schulkin J. *Rethinking homeostasis: allostatic regulation in physiology and pathophysiology*. Cambridge: MIT Press; 2003.
- [38] Wegner DM. Ironic processes of mental control. *Psychol Rev* 1994;11:34–52.
- [39] Freire JG, Gallas JAC. Stern-Brocot trees in the periodicity of mixed-mode oscillations. *Phys Chem Chem Phys* 2011;13:12191–8.
- [40] Freire JG, Gallas JAC. Stern-Brocot trees in cascades of mixed-mode oscillations and canards in the extended Bonhoeffer-Van der Pol and the Fitzhugh–Nagumo models of excitable systems. *Phys Lett A* 2011;375:1097–103.
- [41] Freire JG, Pöschel T, Gallas JAC. Stern-Brocot trees in spiking and bursting of sigmoidal maps. *Europhys Lett* 2012;100:48002.
- [42] Freire JG, Field RJ, Gallas JAC. Relative abundance and structure of chaotic behavior: the nonpolynomial Belousov-Zhabotinsky reaction kinetics. *J Chem Phys* 2009;131:044105.
- [43] Nascimento MA, Gallas JAC, Varela H. Self-organized distribution of periodicity and chaos in an electrochemical oscillator. *Phys Chem Chem Phys* 2011;13:441–6.
- [44] Gallas JAC. Spiking systematics in some CO<sub>2</sub> laser models. *Adv Atomic Molec Opt Phys* 2016;65:127–91.